# Numerical methods for 6-D dynamics simulations in FFAG rings.

**F. Lemuet, F. Méot, A. Verdier**
**Plus, recent step ahead in collab. with M. Aiba**

13 Oct. 2004

**Main topic :**
**3-D simulation of the field in an FFAG radial sector magnet, from its geometrical parameters. Application to multiturn tracking.**

The method is derived from the simulation of large dipoles, as implemented in the 70's in the ray-tracing code Zgoubi for the design of large acceptance spectrometers

**Motivations of this FFAG magnet simulation :**

**• develop an efficient ray-tracing tool for further NuFact FFAG studies - design, tracking**

**• provide field simulation from purely analytical expressions of 3-D field - no field maps, no interpolation !**

**• yield fast, high precision tracking**

**• allow fast optimization of magnet geometry as constrained by machine parameters, using for instance automatic matching procedures**

**Contents**

# 1 The ray-tracing method - Ingredients necessary for magnet simulation

$$\bullet Position\ :\ \vec{R}(M_1)\ \approx \vec{R}(M_0) + \vec{u}(M_0)\,\Delta s + \vec{u}'(M_0)\,\tfrac{\Delta s^2}{2!} + ... + \vec{u}''''''(M_0)\,\tfrac{\Delta s^6}{6!}\ [+...] \qquad (1)$$

$$\bullet Velocity\ :\ \vec{u}(M_1)\ \approx \vec{u}(M_0) + \vec{u}'(M_0)\,\Delta s + \vec{u}''(M_0)\,\tfrac{\Delta s^2}{2!} + ... + \vec{u}''''''(M_0)\,\tfrac{\Delta s^5}{5!}\ [+...]$$

using $\vec{u}' = \vec{u} \times \vec{B}$ (Lorentz equation), $\vec{u}'' = \vec{u}' \times \vec{B} + \vec{u} \times \vec{B}'$ , $\vec{u}''' = ...$ *etc.*

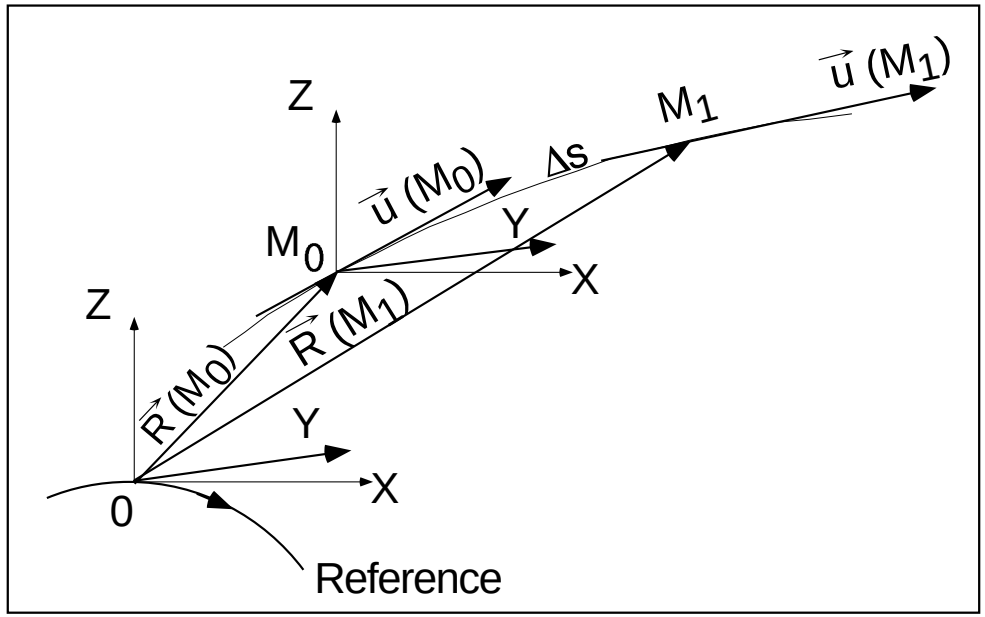


Figure 1: Position and velocity of a particle in the reference frame.

**Note : if spin tracking, then in addition**

$$\bullet\ \vec{S}(M_1) \approx \vec{S}(M_0) + \vec{S}'(M_0)\,\Delta s + ... + S''''(M_0)\frac{\Delta s^4}{4!}\ [+...] \quad \text{using } \vec{S}' = \vec{S} \times \Omega(\vec{u}, \vec{B}),\ \vec{S}'' = ...\ etc. \qquad (2)$$

**Taylor coefficients**

**Four steps are necessary to calculate $\boxed{\vec{B}(s)}$ and its derivatives $\boxed{d^n\vec{B}/ds^n}$ :**

1. **A FFAG sector mid-plane field model of the form**

$$B_z(r,\theta) = B_{z0}\,\mathcal{F}(r,\theta)\,\mathcal{R}(r) \qquad \text{that also yields the field derivatives} \quad \partial^{i+j}B_z/\partial\theta^i\partial r^j \tag{3}$$

   *Obtaining this mid-plane model is the main subject of this talk.*

2. **Next, transform from magnet cylindrical frame into Zgoubi Cartesian frame, using**

$$\partial B_z/\partial X = (1/r)\partial B_z/\partial\theta,\ \ \partial B_z/\partial Y = \partial B_z/\partial r,\ \ \partial^2 B_z/\partial X^2 = (1/r^2)\partial^2 B_z/\partial\theta^2 + (1/r)\partial B_z/\partial r,\ \ etc.$$

3. **$Z$-derivatives and extrapolation off mid-plane yield yield the 3-D $\vec{B}$ model**

$$\boxed{\vec{B}(X,Y,Z), \qquad \partial^{i+j+k}\vec{B}/\partial X^i\partial Y^j\partial Z^k}$$

4. **Eventually, the derivatives $\boxed{d^n\vec{B}/ds^n}$ needed in Eqs. 1 are derived from the above using**

$$\vec{B}'(s) = \sum_i \frac{\partial\vec{B}(X,Y,Z)}{\partial X_i}\,u_i(s)\,, \qquad \vec{B}''(s) = \sum_{ij}\frac{\partial^2\vec{B}(X,Y,Z)}{\partial X_i\partial X_j}\,u_i(s)\,u_j(s) + \sum_i \frac{\partial\vec{B}(X,Y,Z)}{\partial X_i}\,u_i'(s) \ \ et$$

   ($X_{i,j,...},\ i,j,... = 1,3$ stand for $X,\ Y$ or $Z$).

## 2 A former "*DIPOLE*" procedure

**... the FFAG one will be derived from.**
**An analytical dipole mid-plane model $B_z(r,\theta)$ is provided in Zgoubi by the *DIPOLE* procedure,**
**- installed in the code in the early 70's for the design of SPES2 spectrometer at SATURNE (Saclay),**
**- used since then for the design of several large spectrometers :**
**SPES3 and others at SATURNE, SPEG (GANIL, Caen), Kaon-QD (GSI), etc.**

**A regular way of simulating magnetic fields within the limits of "Effective Field Boundaries"(EFB)**
**- also used in other spectrometer codes (e.g., RAYTRACE, S. Kowalski) :**

**GEOMETRY OF A DIPOLE :**

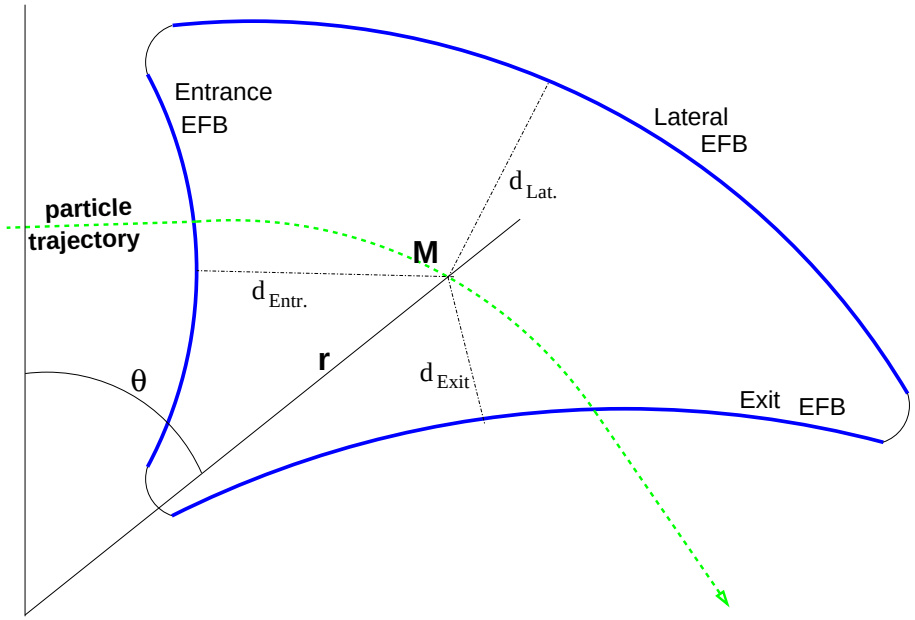


**The field at position $M(r,\theta)$ on the trajectory is calcu**
**lated from the distance of the surrounding EFB's :**
**1. each EFB is responsible of a field form factor tha**
**describes its field fall-off**
**2. the resulting form factor at $M$ is the product of th**
**individual form factors :**

$$\mathcal{F}_i(r,\theta) = \mathcal{F}_{\textbf{Entrance}}(r,\theta)\times\mathcal{F}_{\textbf{Exit}}(r,\theta)\times\mathcal{F}_{\textbf{Lateral}}(r,$$

**That yields a vertical field at $M$ of the form**

$$B_z(r,\theta) = B_{z0}\,\mathcal{F}(r,\theta)\,\mathcal{R}(r)$$

**wherein $\mathcal{R}(r)$ is a possible radial dependence of $B_z$.**

## Example : Design of Elbeck spectrometer SPES3 using *DIPOLE*.

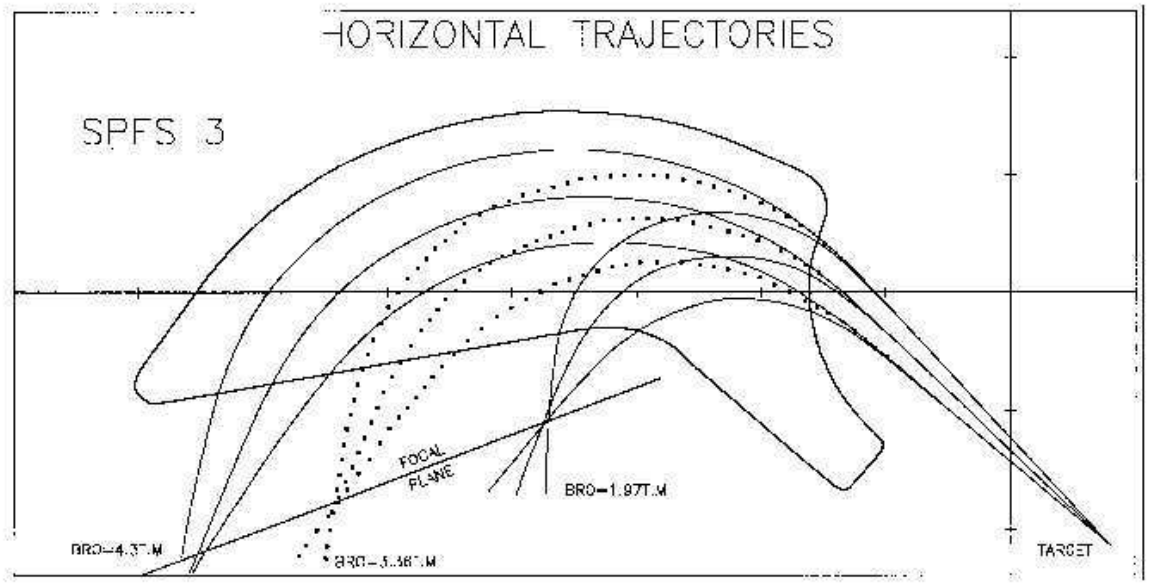


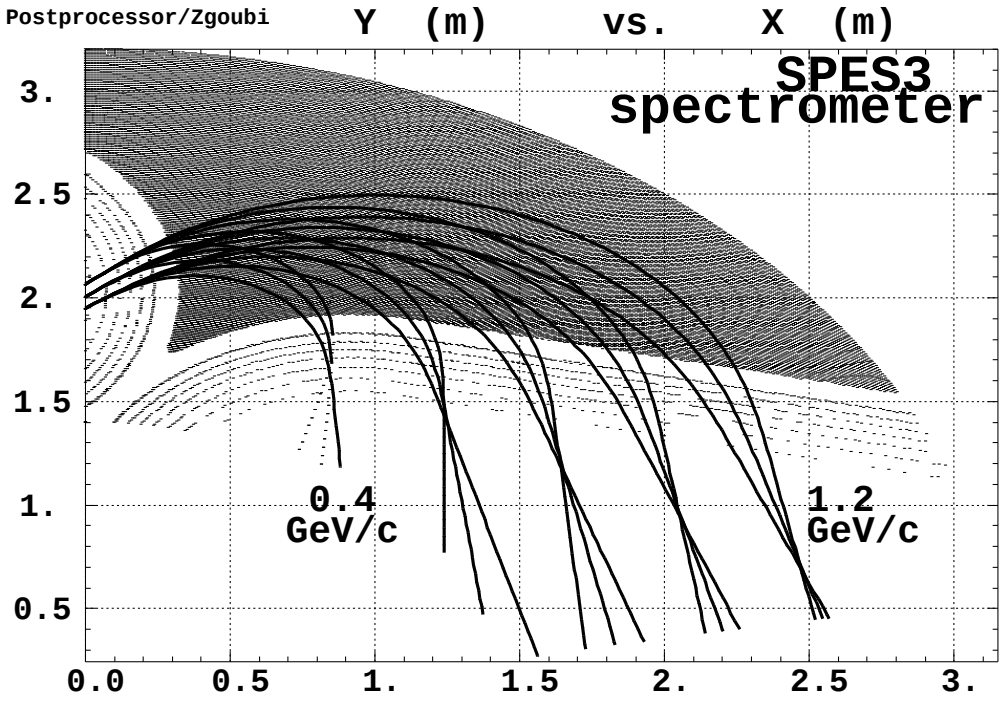


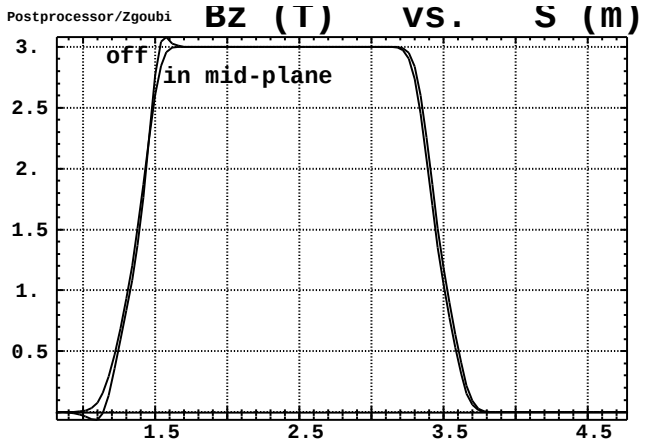


**The construction of SPES3 used the geometrical parameters so optimized by means of "*DIPOLE*" (field form factors determined using POISSON) - no 3-D magnet simulations at that time.**

# Ex. #2 : Design of SPES2 using *DIPOLE*.

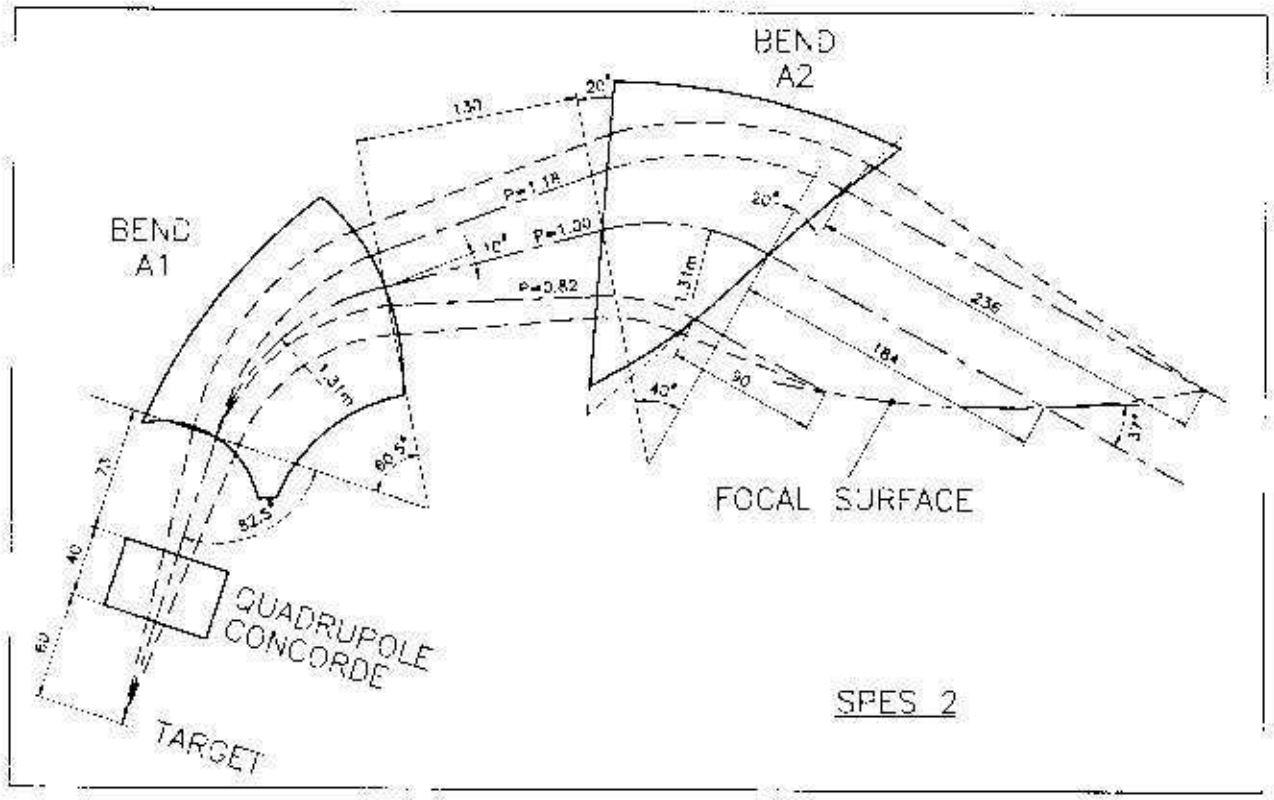


```
***  SPES2  600MEV/C
'OBJET'
2335.
5
.104113721 .832545509 0.104 1.85043641 0. .001
0. 0. 0. 0. 0. 1.
'ESL'
60.
'QUADRUPO'
 0
40.  10. -5.61
0.  0.
6  .1122 6.2671 -1.4982 3.5882 -2.1209 1.723
0.   0.
6  .1122 6.2671 -1.4982 3.5882 -2.1209 1.723
3.
1 0. 0. 0.
'ESL'
27.893
'DIPOLE'           BEND A1
2 0 0
350  200
15.273   0. 0. 0.
107.  50.   131.  70.  180.
46. -1.
4   .14552 5.21405 -3.38307 14.0629 0. 0. 0.
 31.  17.5    -57.24  0.    0.  -57.24
46. -1.
4   .14552 5.21405 -3.38307 14.0629 0. 0. 0.
-32. -10.    -158.    0.    0. -126.
0
25
.3
2
 138.548   -.33161256  144.648 .43827
'ESL'
24.21
'DIPOLE'           BEND A2
2 0 0
350  200
15.2730  0. 0. 0.
78.   39.   131.  60.  210.
46. -1.
4   .14552 5.21405 -3.38307 14.0629 0. 0. 0.
 20.  20.     1.E6   -1.E6    1.E6   1.E6
46. -1.
4  .14552  5.21405  -3.38307  14.0629 0. 0. 0.
-20.  20.    -350.  -26.5  20.5  800.
0
25
.3
2
 138.548   -.331612558   138.716 .33451
'END'
```

**In the case of the two SPES2 large acceptance dipoles "A1" and "A3", the optimization of the geometrical parameters was also accomplished using "*DIPOLE*". Their behavior was fully satisfying - the spectrometer did work fine !**

# 3 An $N$-uplet magnet procedure. Simulation of FFAG radial sector triplet

**GEOMETRY/FIELD FOR ONE DIPOLE :**

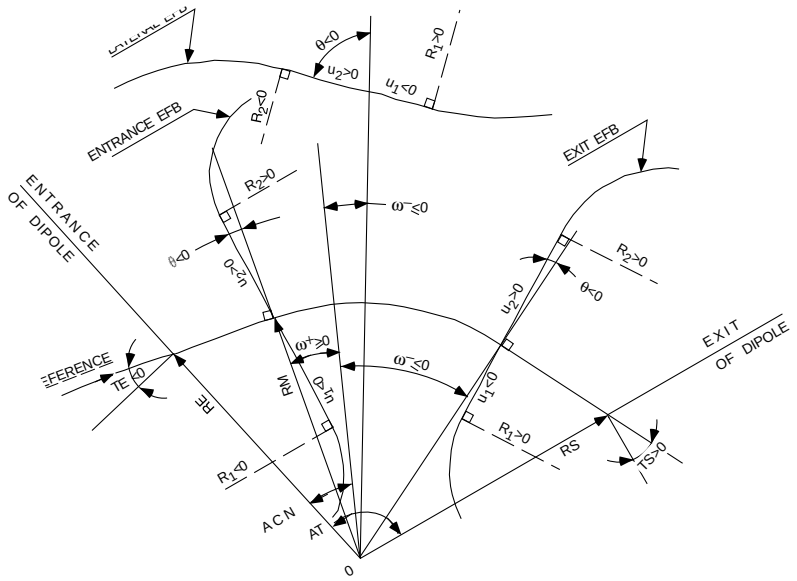


When alone, a dipole is encompassed in the magnetic field region defined by the angle $AT$. The dipole geometrical parameters yield the mid-plane vertical field :

$$B_{zi}(r,\theta) = B_{z0,i}\,\mathcal{F}_i(r,\theta)\,\mathcal{R}_i(r)$$

by using

$$\mathcal{R}_i(r) = (r/R_{0,i})^K$$

and

$$\mathcal{F}_i(r,\theta) = \mathcal{F}_{\text{Entrance}}(r,\theta) \times \mathcal{F}_{\text{Exit}}(r,\theta) \times \mathcal{F}_{\text{Lateral}}(r,\theta$$

simulating the effect of EFB's $\longrightarrow$ discussed next slide.

**GEOMETRY/FIELD FOR A SECTOR TRIPLET :**

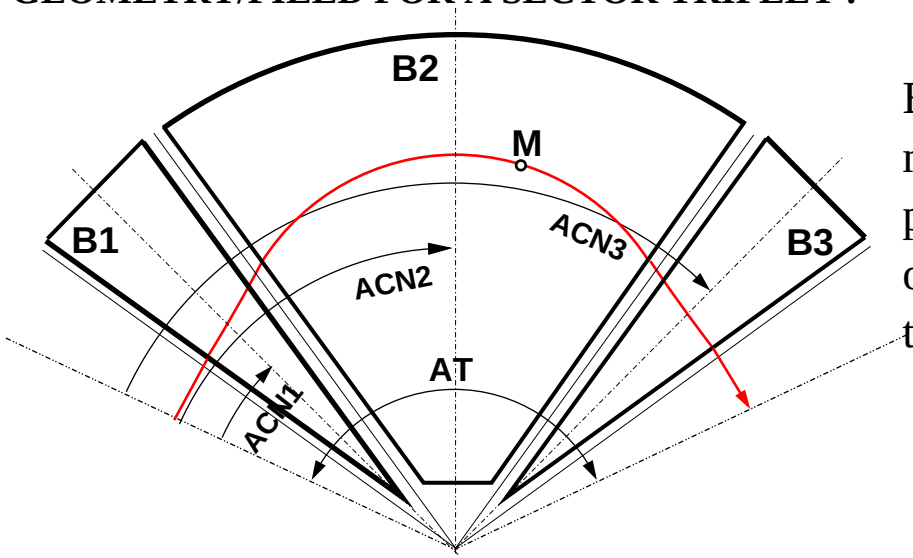


Basically, N=3 (here) dipoles are encompassed in the magnetic field region defined by the angle $AT$, they are positioned by $ACNi$. Obtaining the total field is a matter of summation over the $N$ neighboring dipoles (not more than a trick)

$$B_z(r,\theta) = \sum_{i=1}^{N} B_{zi}(r,\theta) = \sum_{i=1}^{N} B_{z0,i}\,\mathcal{F}_i(r,\theta)\,\mathcal{R}_i(r) \quad (4$$

$$\text{Derivatives : } \frac{\partial^{i+j}\vec{B}_z(r,\theta)}{\partial\theta^i\partial r^j} = \sum_{i=1,N} \frac{\partial^{i+j}\vec{B}_{zi}(r,\theta)}{\partial\theta^i\partial r^j} \quad (5$$

# Simulation of fi eld fall-offs

**Field fall-off at an** $EFB$ **(*Entrance, Exit*** $EFB$**) is modeled by**

$$\mathcal{F}_{EFB}(d) = (1+\exp[P(d)])^{-1}\,, \quad P(d) = C_0 + C_1\frac{d}{g} + C_2\left(\frac{d}{g}\right)^2 + \ \ldots\ + C_5\left(\frac{d}{g}\right)^5$$

- $d(r,\theta)$ **is the distance to the** $EFB$

- **Possible gap variation is accounted for :** $g$ **is homogeneous to the gap, e.g.,**

  $g(r) = g_0(R_0/r)^K$ **(pole shaping),**
  **or**
  $g = C^{\underline{\mathbf{te}}}$ **(coil shaping)**

- **coefficients** $C_0 - C_5$ **determine the shape of the field fall-off** (can be determined from prior POISSON or TOSCA calculations for instance)

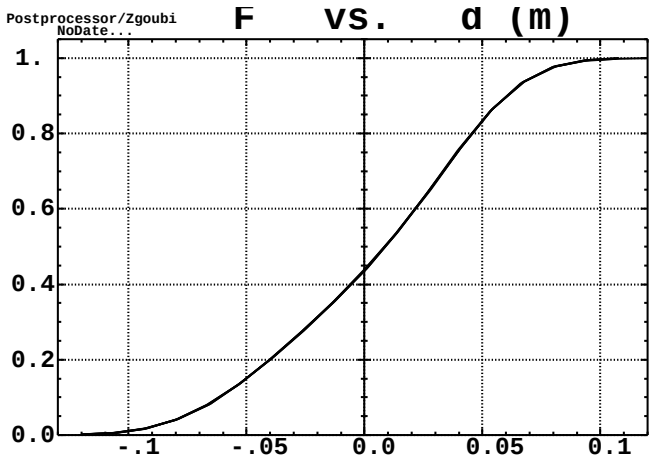


**Figure 2:** Fringe field $\mathcal{F}_{EFB}$ as a function of distance $d$ (gap $g = 8$ cm, $C_0 = 0.1455$, $C_1 = 2.2670$, $C_2 = -0.6395$, $C_3 = 1.1558$, $C_4 = C_5 = 0$).

# Calculation of the mid-plane field derivatives

**Two different methods have been implemented to calculate the field derivatives in the median plane, based on**

**• either from analytical expressions explicitely in the code, as obtained from differenciation of P(d,g) in the fringe field model,**
**• or numerical interpolation**

**The first method has the merit of insuring better symplecticity and faster tracking.**

**The second method has the merit of facilitating easy possible changes to the source code so as to modify the mid-plane magnetic field model $B_z(r,\theta)$.**

*Numerical interpolation*

**In this case the expression $B_z(r,\theta)$ in Eq. 4 is computed at the $n * n$ nodes ($n = 3$ or $5$ in practice) of a "flying" interpolation mesh in the median plane centered on the actual particle position. A polynomial interpolation yields the derivatives.**

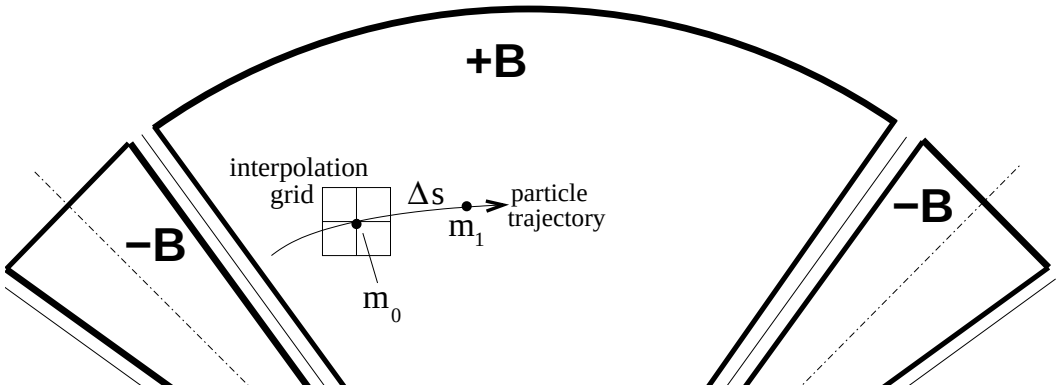

# Numerical results : Field along an arc of a circle in a radial sector :

$$B_z(r,\theta) = \sum_{i=1,N} B_{zi}(r,\theta) = \sum_{i=1,N} B_{z0,i}\,\mathcal{F}_i(r,\theta)\,\mathcal{R}_i(r)$$

**MID-PLANE FIELD IN FFAG SECTOR TRIPLET :** **OFF MID-PLANE, CLOSE TO POLE :**

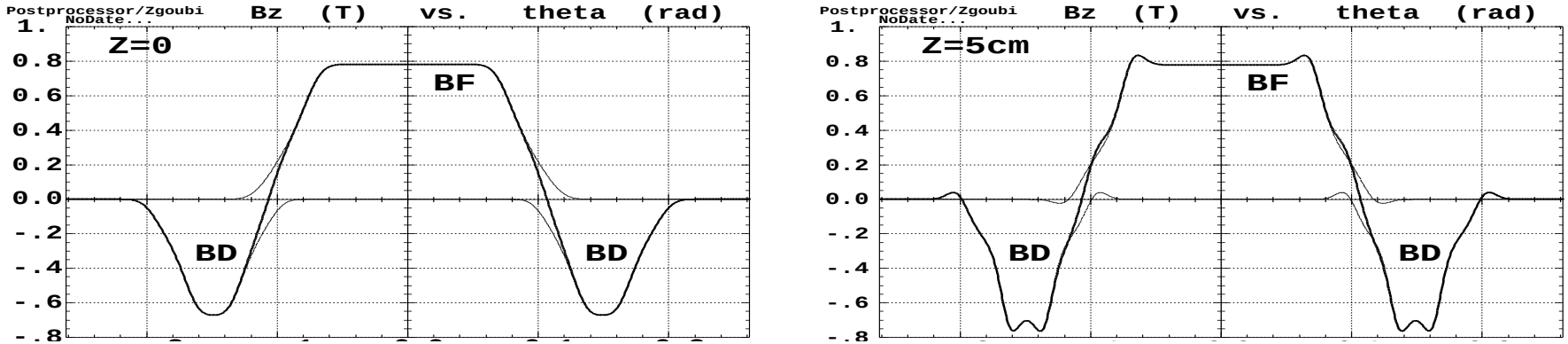


Figure 3: $B_z(r_0,\theta,z)$ (Eq. 4) at traversal of the 30 degrees aperture FFAG triplet in the 50 MeV closed orbit region and for either $z = 0$ (left plot) or $z = 6$ cm as obtained by off mid-plane extrapolation (right). On both plots the thick curve represents the full field, as obtained by superposition of the separate contributions of each one of the three dipoles represented by the thin curves.

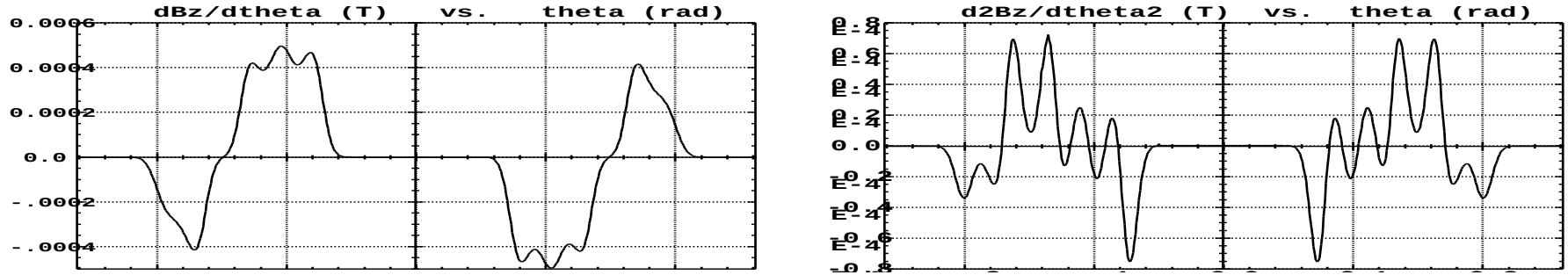


Figure 4: Mid-plane derivatives $\partial B_z(r,\theta)/\partial\theta$ (left plot) and $\partial^2 B_z(r,\theta)/\partial\theta^2$ (right) (Eq. 5) along a closed orbit ($r \approx 4.87$ m). *Note :* these plots show that the ray-tracing integration step $\Delta S$ (and also the mesh size in the case field maps would be used to simulate such magnets) *has to be small*.

## 4 Application : the KEK 150 MeV proton FFAG ring

Goal : try to show that the method works fi ne...

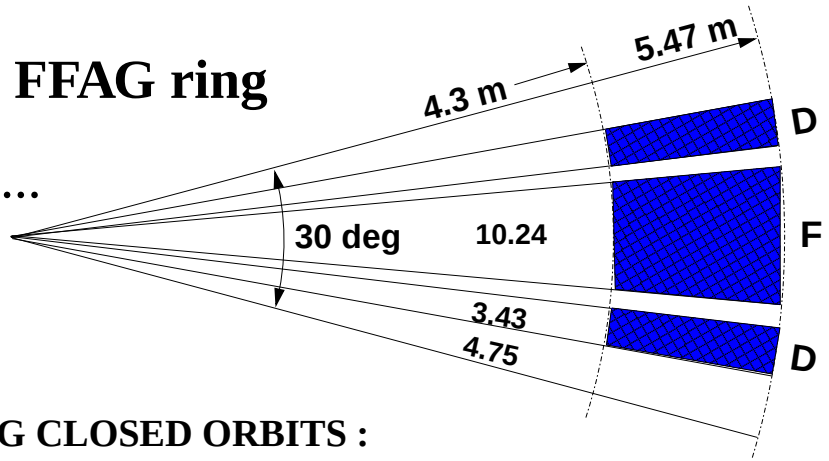


**MID-PLANE FIELD ALONG CLOSED ORBITS :**

**FIELD COMPUTED ANALYTICALLY**

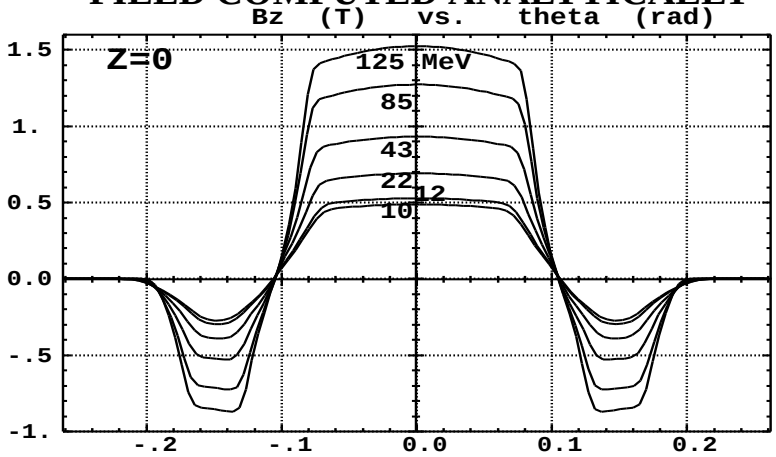


**FIELD COMPUTED FROM TOSCA 3-D MAP**

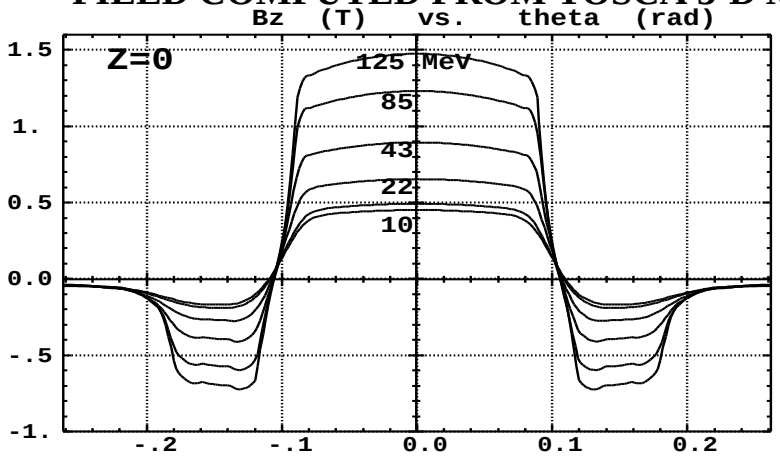


The field in the case of the geometrical method has been tuned so as to yield results as close as possible to the TOSCA map case. This was done using two constraints :

1/ closed orbit must be the same as in the TOSCA map case at 43 MeV (value chosen because it is about half-way between $r_{min}$ and $r_{max}$),

2/ same horizontal and vertical tunes with both methods.

• Condition 1/ yields BF, and condition 2/ yields BF/BD ratio. •

• *Remark :* no effort was made to have the analytical field shape closer to TOSCA case in the BD and drift regions. This would be possible by matching of the $C_i$ fringe field coefficients •

**CLOSED ORBITS IN CELL :**

**GEOMETRICAL MODEL**

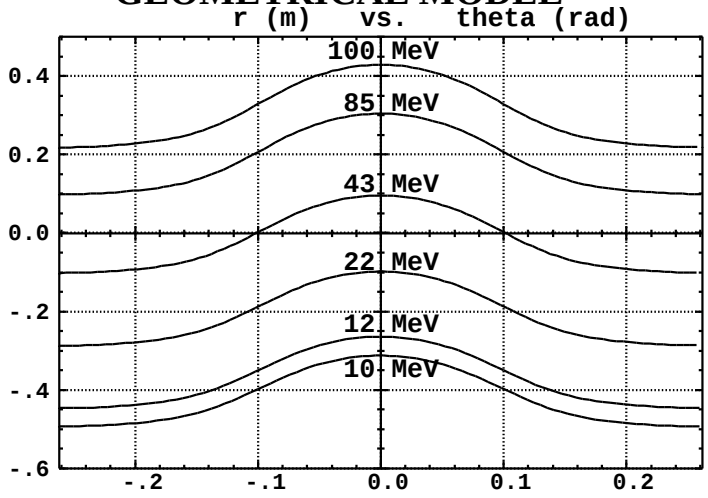


**FOR COMP.: TOSCA 3-D MAP**

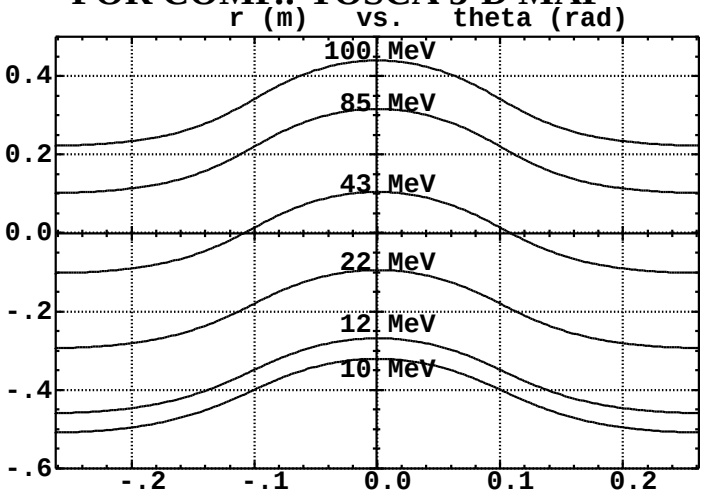


One observes a slightly larger overall excursion in the TOSCA map case, a kind of effect that could be obtained with a $K$ value slightly smaller than 7.6 (that of the geometrical model).

**TUNES (full turn, 12 cells) :**

$\nu_r$

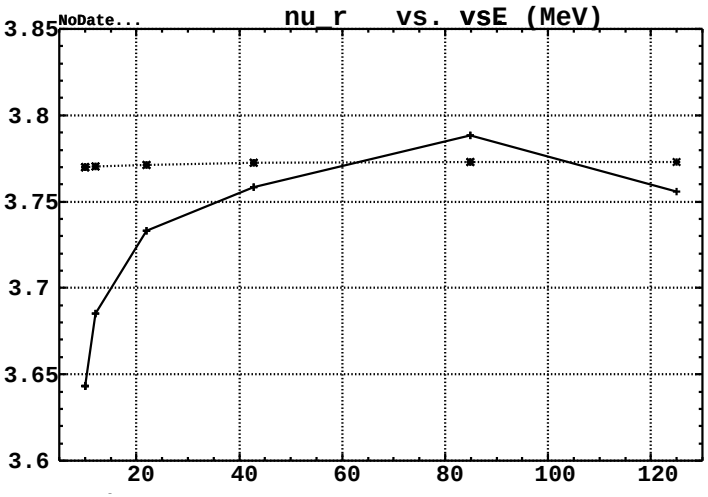


$\nu_z$

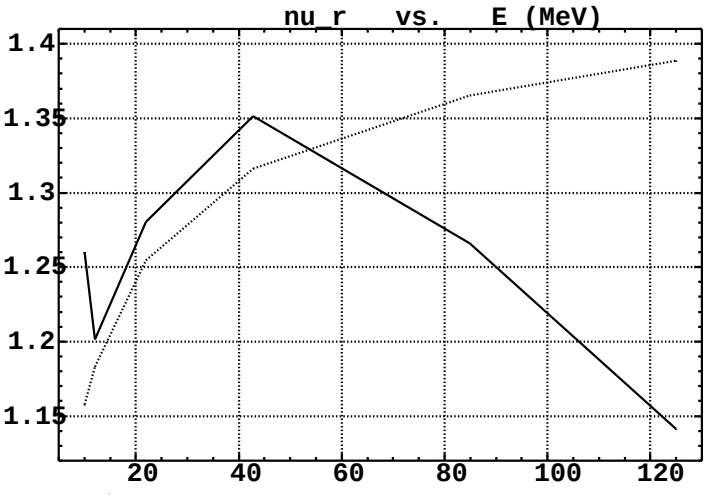


**Machine tunes. Dashed lines are from the geometrical method, solid lines are from TOSCA map.**

## BEAM ENVELOPES

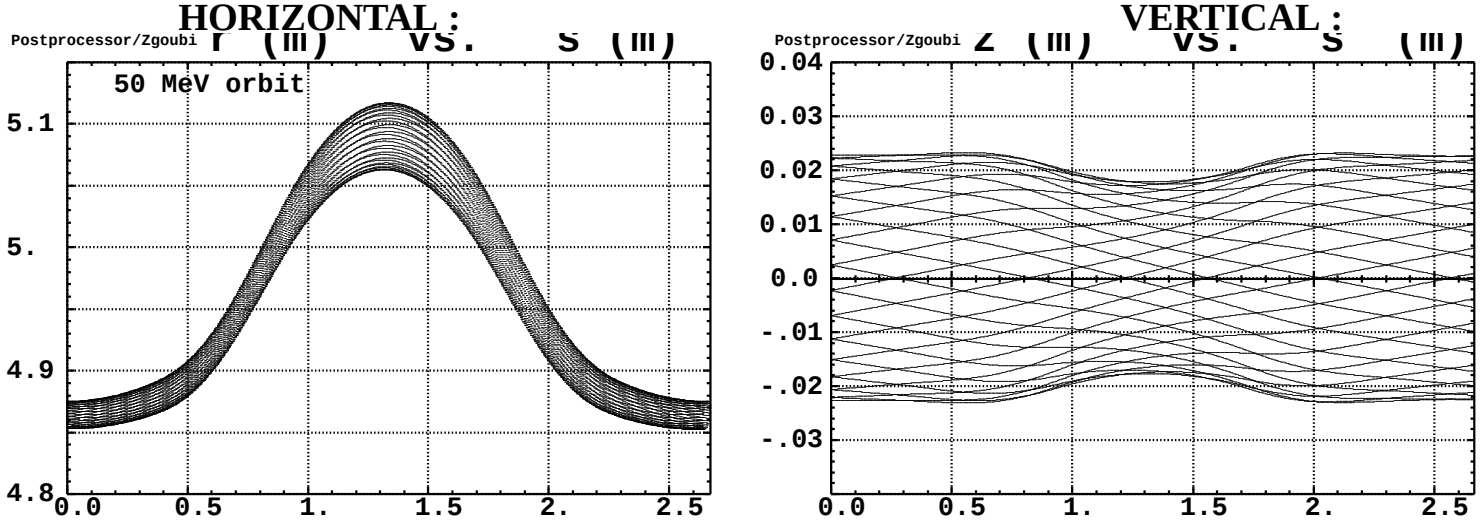


Figure 5: Beam tubes in a cell, generated by 40-turn tracking of particles launched on the invariants respectively $\epsilon_x = 200\,\pi$ mm.mrad, $\epsilon_z = 0$ (left plot) and $\epsilon_x = 0$, $\epsilon_z = 200\,\pi$ mm.mrad (right plot).

## BETA VALUES

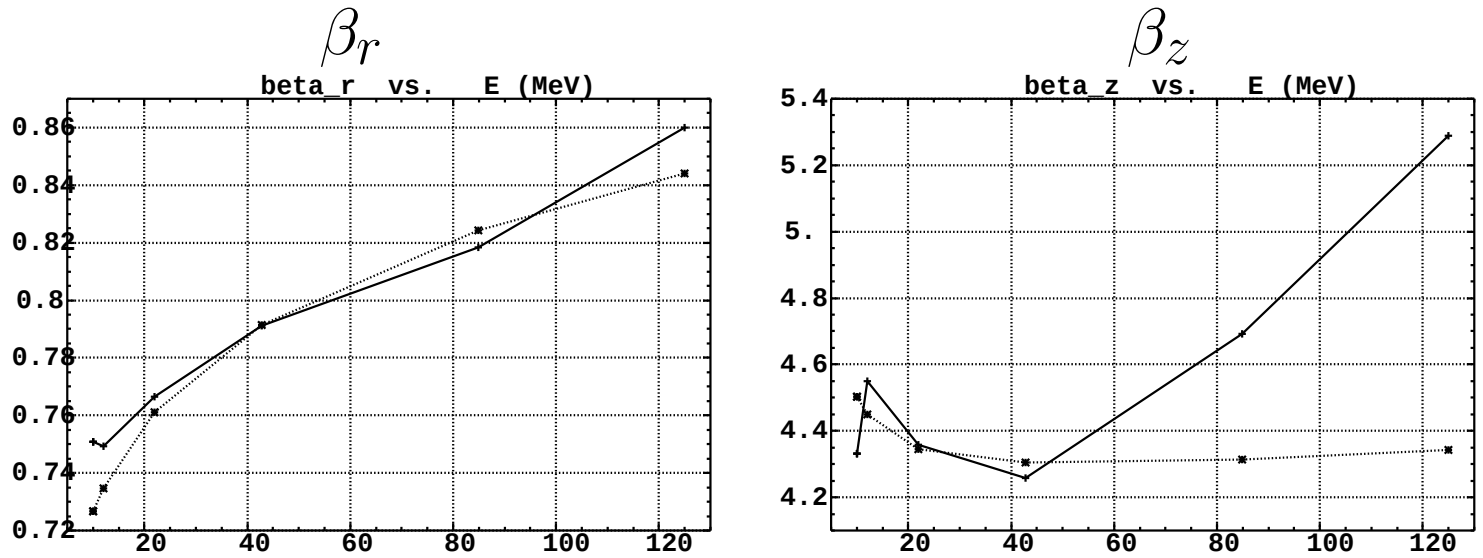


beta functions at center of drift. Dashed lines are from the geometrical method, solid lines are from TOSCA map.

# Stability limits

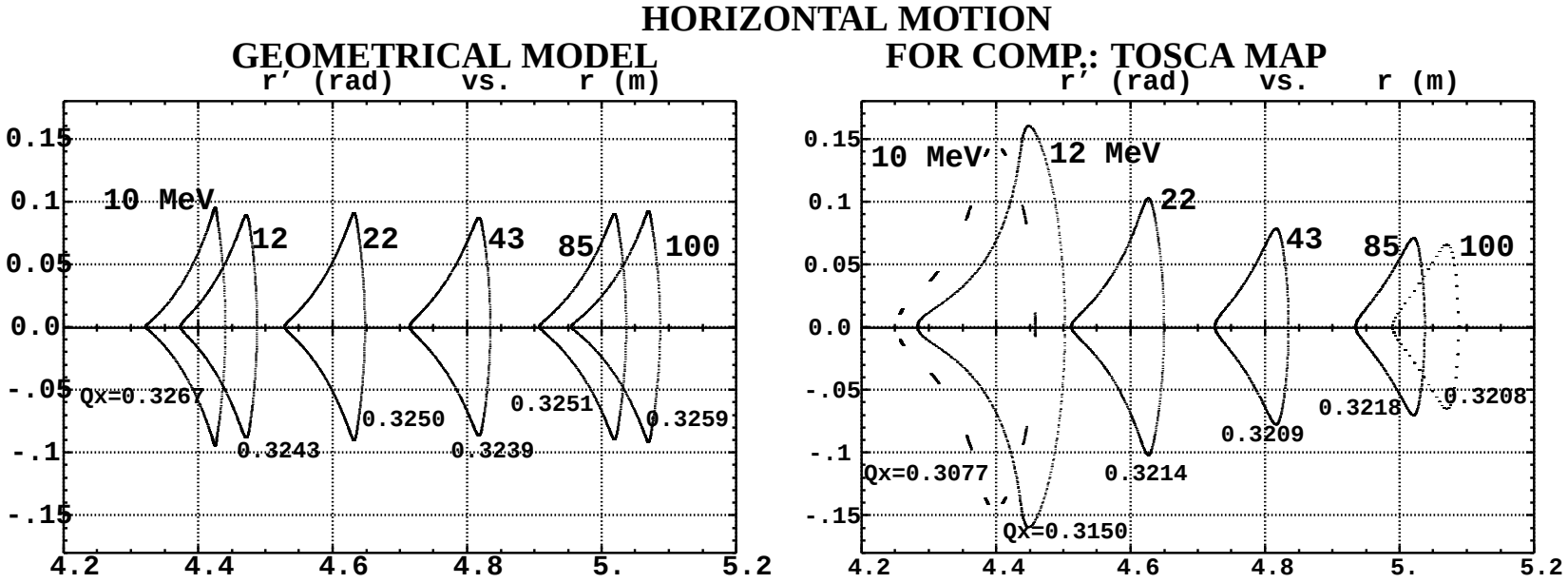


The limits of stable motion for 5 energies, with better than $\Delta r = \pm 0.1$ mm accuracy.

# Synchrotron motion, Zero synchronous phase

**Characteristics of RF after [KEK Pubs.] :** $\hat{V} = 19$ **kV,**
**RF frequency after previous ray-tracing results.**

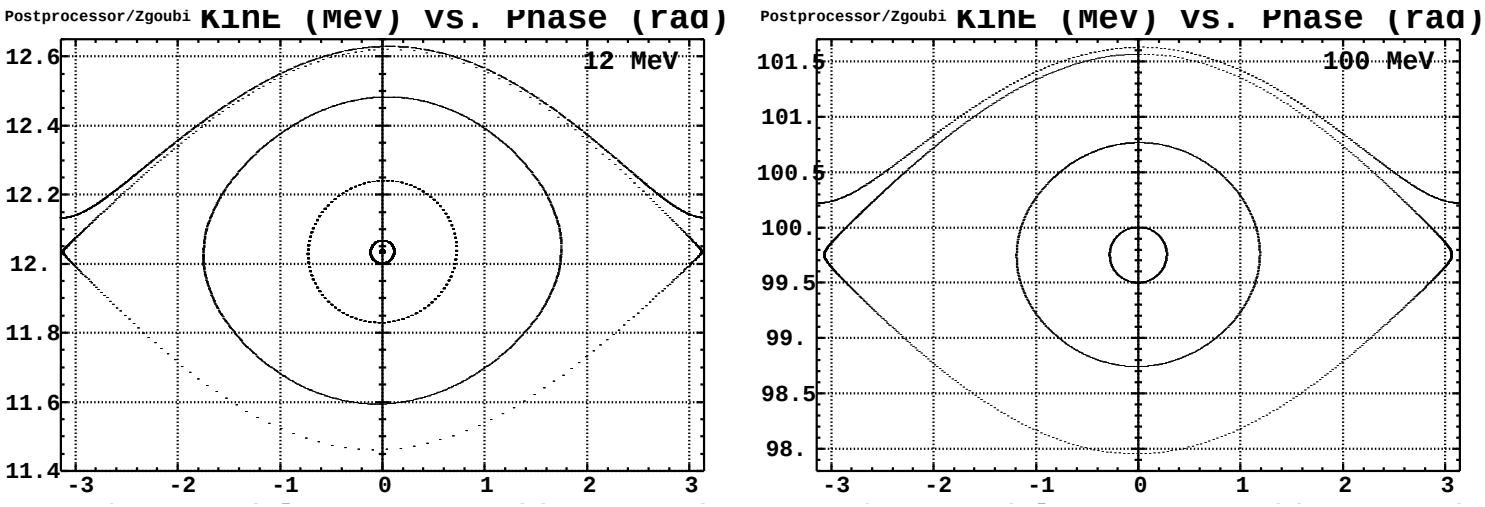


Figure 6: Synchrotron motion in $12$ MeV and in $100$ MeV region (left and right plots, respectively), harmonic 1, zero synchronous phase - about $1000$ turns.

$$\eta = 1/\gamma^2 - \alpha, \quad f_s = \Omega_s/2\pi = \frac{c}{\mathcal{L}}\left(\frac{h\eta\cos\phi_s q\hat{V}}{2\pi E_s}\right)^{1/2}, \quad \pm\frac{\Delta p}{p} = \pm\frac{1}{\beta_s}\left(\frac{2q\hat{V}}{\pi h\eta E_s}\right)^{1/2}.$$

Table 1: Parameters of synchrotron motion, from ray-tracing ("num.") with comparison to theory ("th.").

| E (MeV) | $\eta = d\mathcal{L}/\mathcal{L}/dp/p$ | | $\nu_s$ | | bucket height ($\pm\Delta p/p$) | |
|---|---|---|---|---|---|---|
| | num. | th.$^{(a)}$ | num. | th.$^{(b)}$ | num.$^{(c)}$ | th.$^{(d)}$ |
| 150 | 0.6293 | 0.6293 | 0.00261 | 0.002610 | 0.0083 | 0.008295 |
| 100 | 0.7027 | 0.7026 | 0.00338 | 0.003341 | 0.0095 | 0.009509 |
| 50 | 0.7874 | 0.7873 | 0.00493 | 0.004942 | 0.0126 | 0.012554 |
| 12 | 0.8611 | 0.8609 | 0.01042 | 0.010448 | 0.0242 | 0.024272 |

**Full acceleration cycle, from 12 to 150 MeV is now experimented.**

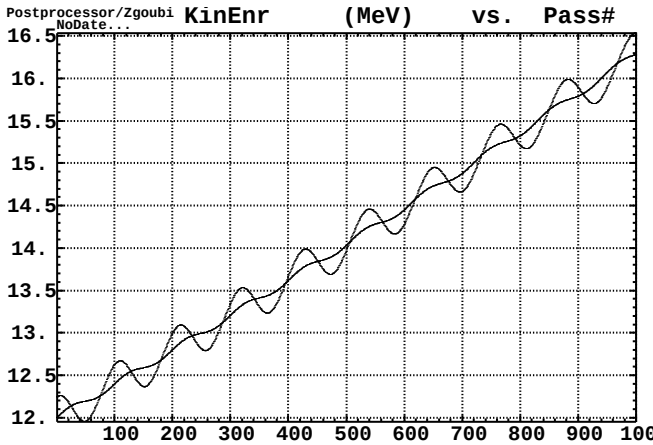


**Characteristics of the acceleration after [KEK Pubs.] :**

- $\hat{V} = 19$ **kV,**
- $\phi_s = 20$ **degrees**

**RF frequency after previous ray-tracing results.**

Sample synchrotron motion. 2 particles : $r_0 =$ and respectively E=12 MeV and 12 MeV+1%.

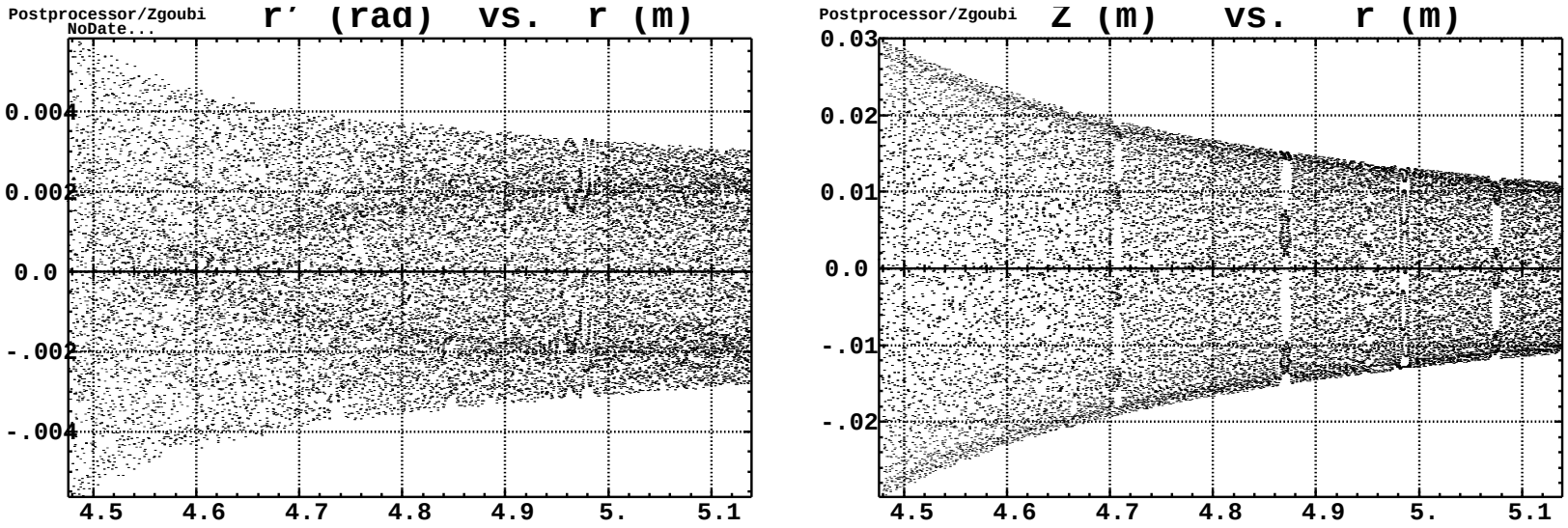


Figure 7: Acceleration from 12 MeV to 150MeV about, $\phi_s = 20$ degrees, $r_o = r_{c.o.}$(12 MeV), $z_0 = 3$ cm. Horizontal phase-space (right) and vertical motion (vs. $r$) ; observation is at center of drift.

# 5 Application : Phase rotation

**In PRISM, $p_0 = 68$ MeV/c $\pm$20%. E$\approx 20 \pm 7$ MeV**

**Working hypothesis : the earlier design with 8 cells. Design/geometrical parameters as in publications, except for : only one cavity,**

**For simplicity just 5 particles are tracked, representative of the momentum span.**

**No optimization has been done, just want to show that the geometrical method for 3-D field simulation can be applied starightforwardly, from simply the geometrical parameters of the DFD triplet.**

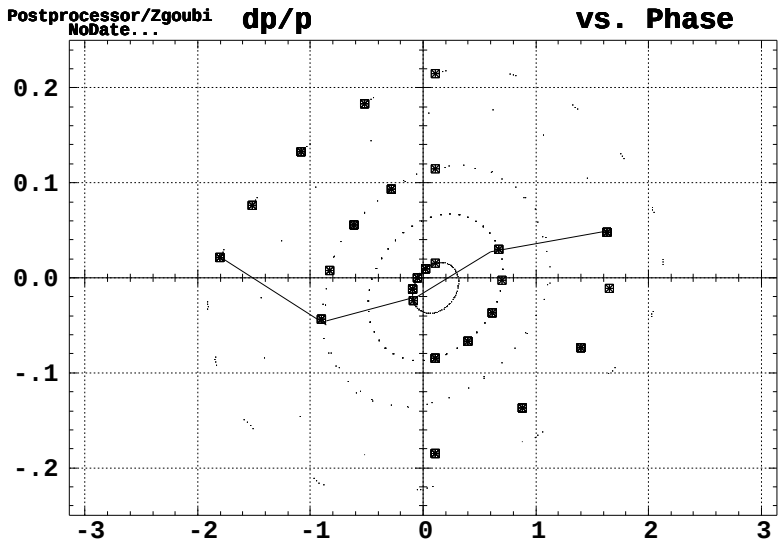


**5 first turns (of a 400-turn tracking). The initial beam is the upright one in the dp-phi space, the solid line shows the final beam.**

```
 constant  gap :                                        variable  gap   ($\alpha$(5/r)^3*6.3cm)

p/p0       1-Q_x / 1-Qz            beta_x / z          p/p0      1-Q_x / 1-Qz
1.2     0.591252 / 0.665596      0.331 / 1.6141.2      1.2    0.611478 / 0.584989
1.1     0.590575 / 0.673290      0.327 / 1.6011.       1.1    0.611109 / 0.609725
1.      0.589929 / 0.680048      0.322 / 1.5851.       1.     0.610565 / 0.639506
.9      0.589110 / 0.688629      0.317 / 1.569.9       .9     0.609959 / 0.674098
.8      0.588170 / 0.698624      0.311 / 1.551.8       .8     0.609184 / 0.715739
```

# Zgoubi data file, PRISM

```
  'OBJET'   * c.o., constant Gap *                                                    1
  226.8235847      68MeV/c muon
  2     5  1
  499.377    0.    0.  0. 0.  1.2     'b'
  492.188    0.    0.  0. 0.  1.1     'a'
  484.4444    0.    0.  0. 0.  1.     'o'
  476.020    0.    0.  0. 0.  .9     'o'
  466.78    0.    0.  0. 0.  .8     'c'
  'FFAG'
  3   45.     500.                        NMAG, AT=tetaF+2tetaD+2Atan(XFF/R0), R0
  ---
  | 18.17   0.  -0.717  5.                    mag 1 : ACNT, dum, B0, K
  | 6.3  0.                                  EFB 1 : lambda, gap const/var=0/>0
  |4  .1455   2.2670  -.6395  1.1558  0. 0.  0.
  | 1.23 0.    1.E6  -1.E6  1.E6  1.E6
  | 6.3  0.                                  EFB 2
D | 4  .1455   2.2670  -.6395  1.1558  0. 0.  0.
  |-1.23  0.    1.E6  -1.E6  1.E6  1.E6
  | 0. -1                                    EFB 3 : inhibited by iop=0
  | 0  0.      0.      0.      0.      0. 0.  0.
  | 0.  0.   0.    0.    0. 0.
  ---
  | 22.5   0.   3.2    5.                    mag 2 : ACNT0.3927rad, m, B0, K,dummies
  | 6.3  0.                                  EFB 1
  | 4  .1455   2.2670  -.6395  1.1558  0. 0.  0.
  | 3.   0.    1.E6  -1.E6  1.E6  1.E6
F | 6.3  0.                                  EFB 2
  | 4  .1455   2.2670  -.6395  1.1558  0. 0.  0.
  |-3   0.    1.E6  -1.E6  1.E6  1.E6
  | 0. -1                                    EFB 3
  | 0  0.      0.      0.      0.      0. 0.  0.
  | 0.  0.   0.    0.    0. 0.
  ---
  |26.83  0.  -0.717  5.                    mag 3 : ACNT, dum, B0, K
  | 6.3  0.                                  EFB 1
  | 4  .1455   2.2670  -.6395  1.1558  0. 0.  0.
  | 1.23 0.    1.E6  -1.E6  1.E6  1.E6
D | 6.3  0.                                  EFB 2
  | 4  .1455   2.2670  -.6395  1.1558  0. 0.  0.
  |-1.23  0.    1.E6  -1.E6  1.E6  1.E6
  | 0. -1                                    EFB 3
  | 0  0.      0.      0.      0.      0. 0.  0.
  | 0.  0.   0.    0.    0. 0.
  ---
  0     2  125.              KIRD anal/num (=0/2,25,4), resol(mesh=step/resol)
  .5                          integration step size (cm)
  2   0.  0. 0. 0.
  --- 8 such FFAG set of data
  'CAVITE'             CAVITY    (only one, 2.2 MV)
  6
  5e6   20.       f0 (Hz),  starting synch Ekin W_s0 (eV)
  2200000.  0.                      Vp (V),  phis (rad)
  'REBELOTE'                                                                        8
  99  0.1 99
  'END'                                                                             9
```

# 6 Application : 8 to 20 GeV isochronous ring

**Magnetic field in bd, BF and BD.**
**The lower plot shows the field in a cell along the 20, 14, 11, 9.5 and 8 GeV closed orbits.**

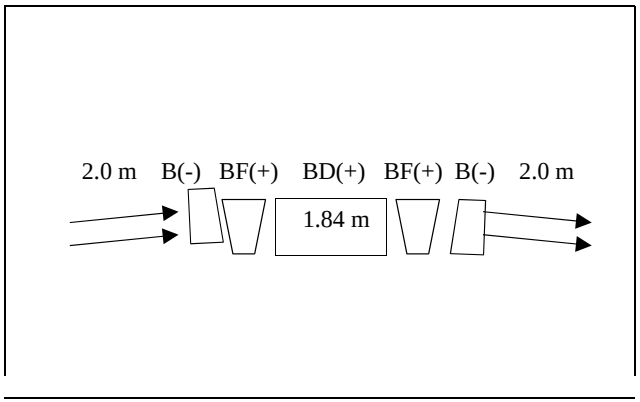


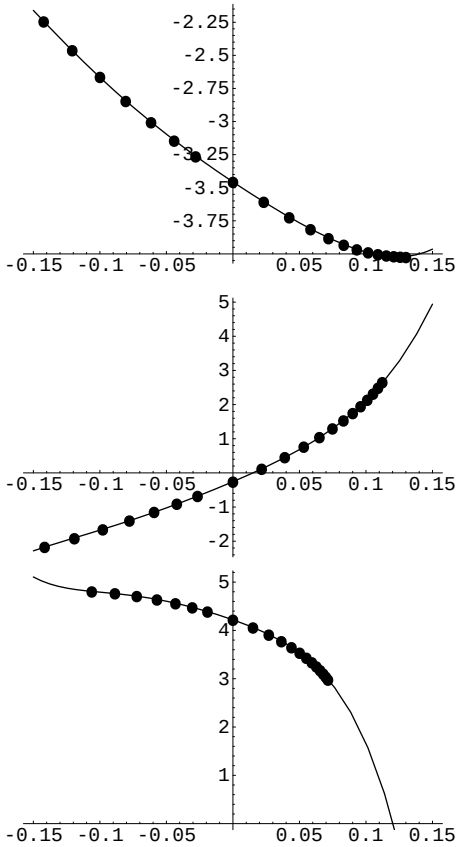


**G. Rees design.**
**Needs precision tracking : the isochronism has to be controlled at a $10^{-6}$ precision.**

**It means accuracy is necessary on**
**- the description of magnetic field in optical elements,**
**- ray-tracing.**

$$B_{bd}(x) = -3.45623 - 6.689211\,x + 9.403200\,x^2 - 7.623605\,x^3 + 360.3808\,x^4 + 1677.7968\,x^5$$

$$B_{BF}(r) = -0.25776 + 16.62046\,r + 29.73987\,r^2 + 158.65762\,r^3 + 1812.1753\,r^4 + 7669.5302\,r^5$$

$$B_{BD}(x) = 4.22034 - 9.65952\,x - 45.4722\,x^2 - 322.1230\,x^3 - 5364.3096\,x^4 - 27510.421\,x^5$$

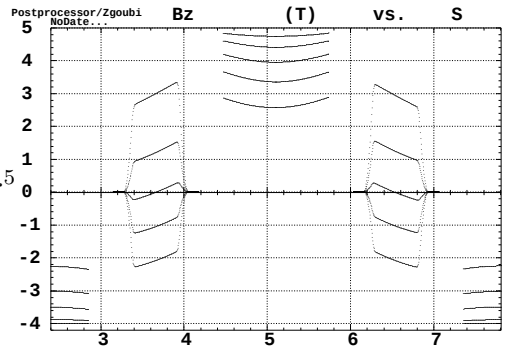

# Stability limits

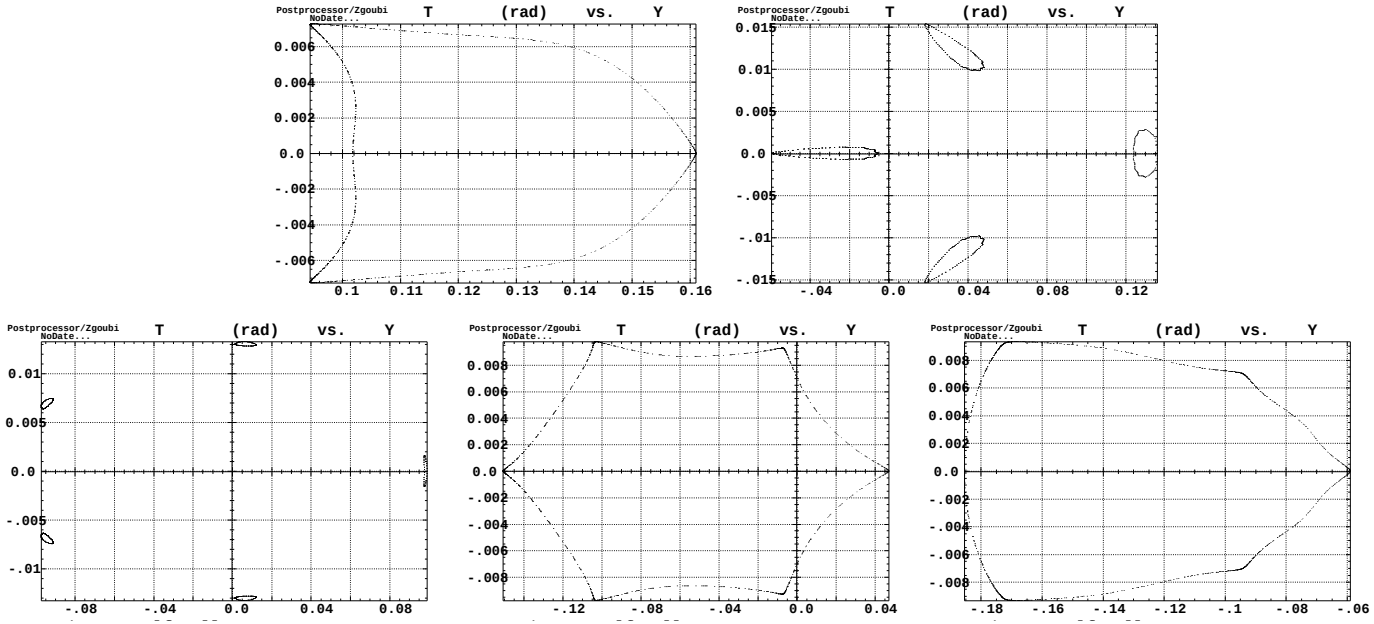


Figure 8: 1000-cell, stability limits of pure horizontal motion, at better than 0.1 cm precision.

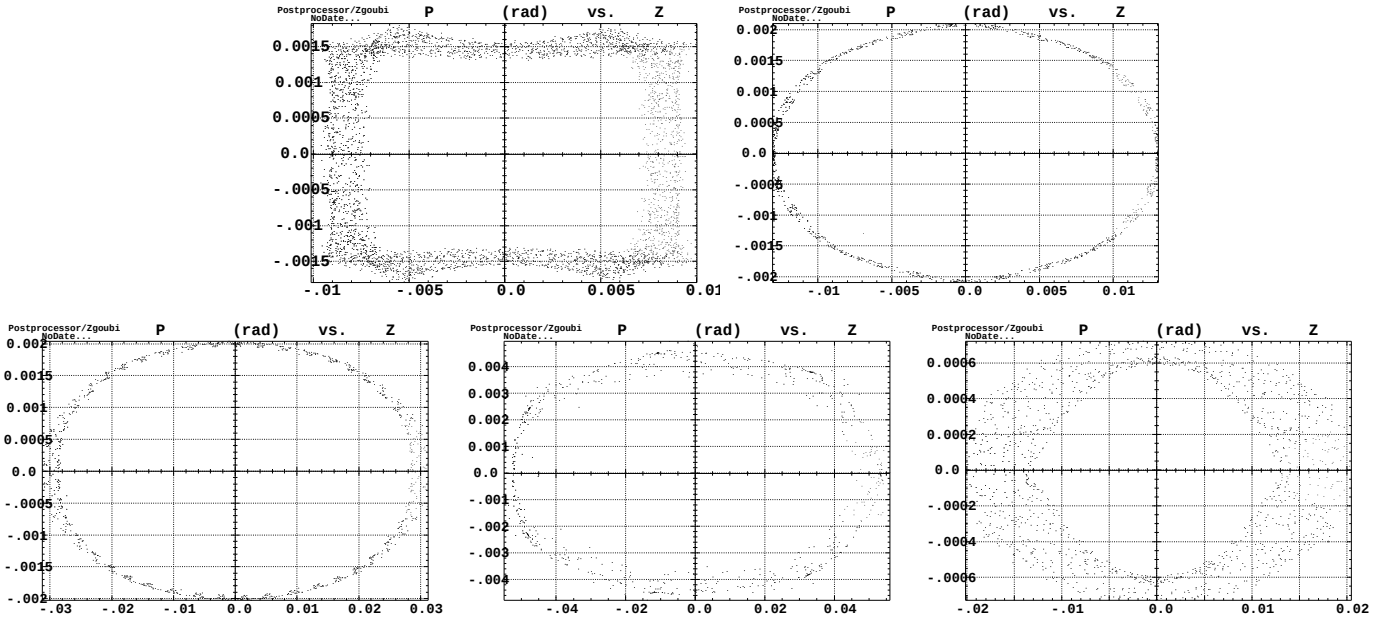


Figure 9: 1000-cell or more, vertical motion stability limits, at better than 0.1 cm precision.

# Amplitude detuning

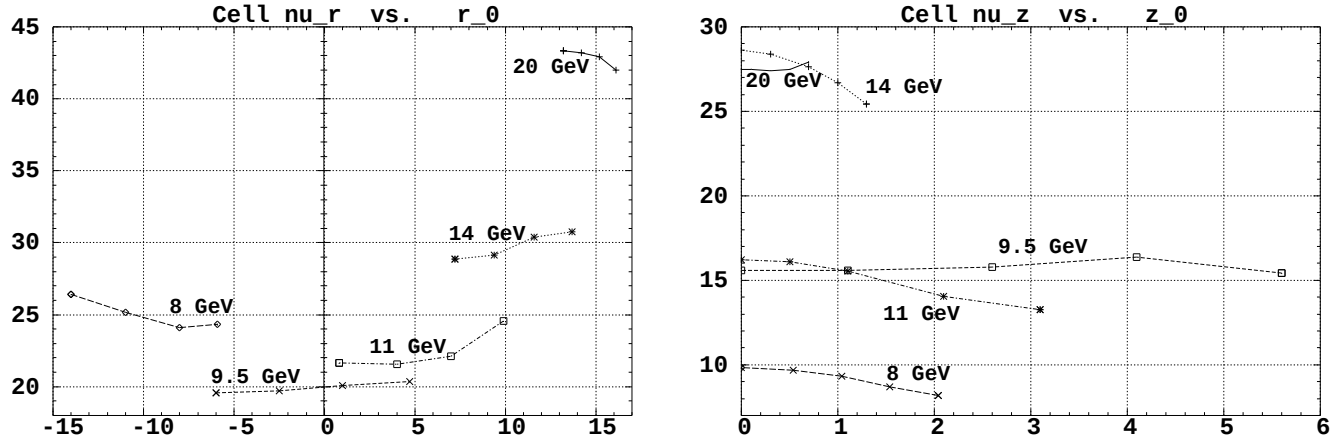


Figure 10: Amplitude detuning. Left : pure radial motion, with for each energy, $x_0$ varied from closed orbit position to maximum stable amplitude. Right : axial motion, with for each energy, $z_0$ varied from zero to maximum stable amplitude while $x \equiv x_{c.o.}$ always.